On the Realization of First-Order Current-Mode AP/HP Filter

Worapong TANGSRIRAT

Faculty of Engineering, King Mongkut's Institute of Technology Ladkrabang (KMITL), Bangkok 10520, Thailand

drworapong@gmail.com

Abstract. *A compact circuit topology for the realization of the current-mode first-order allpass (AP) and highpass (HP) filters is described. The proposed circuit contains a minimum number of components, i.e., eight bipolar transistors, one grounded capacitor, and one biasing current source. The advantages of this circuit are the use of only grounded capacitor as a passive element, the electronic tunability of its parameters and its potential for low-voltage operation. Owing to the pole frequency of the filter circuit is normally dependent on temperature; a low-voltage translinear–based current source circuit for temperature compensation is also suggested. Some simulation results achieved through PSPICE program and experimental test results are also reported, which demonstrate the effectiveness of the proposed circuit.*

Keywords

First-order filter, allpass (AP), highpass (HP), current-mode, integrated circuit.

1. Introduction

First-order filters are one of the important circuit blocks and their use may be found in a variety of analog signal processing applications, such as, feedback control, high-order filter design, and many other engineering applications in the field of instrumentation and telecommunication. As a result of the well-known advantages of current-mode operation, a number of current-mode first-order filters have been developed in the literature [1]-[11]. Traditionally, they were implemented using active building blocks, such as, second-generation current conveyor (CCII), four-terminal floating nullor (FTFN), current feedback operational amplifier (CFOA) and current differencing transconductance amplifier (CDTA). However, the internal structures of these active elements typically involve larger number of transistors, resulting in the high-frequency limitation of the filters. Also, the complexity of the active building blocks dissipated considerable power, and occupied a large chip area. To reduce the power dissipation and chip area, several current-mode first-order filter realizations based on the use of transistor-level circuit were reported [12]-[17]. In [12] and [13], current-mode first-order AP filters including a floating capacitor have been described. The resistorless universal first-order filter in [14] contains twelve of bipolar transistors, one grounded capacitor and four current sources. Types of filter response can be obtained only by changing the values of current sources. The filter of [15] employs four passive components, and requires passive component matching conditions. Moreover, it also requires additional active elements for output current sensing. The work in [16] proposed a resistor-free realization of an active-only voltage-mode first-order AP filter using four NMOS transistors and five biasing current sources. However, active component matching condition is required. Although an interesting circuit configurations for realizing first-order AP filter based on log-domain technique were recently presented in [17], the circuits still contain a large number of active components, i.e., ten bipolar transistors, one grounded capacitor, and seven current sources.

In this paper, a simple bipolar technology-based filter topology that can simultaneously realize both current-mode first-order AP and HP current responses with electronic tuning property is presented. This topology employs eight transistors, one grounded capacitor, and one biasing current source, instead of complex active elements. Since the proposed circuit is resistorless, it provides very useful advantages from integrated circuit implementation viewpoint. Its pole frequency (f_o) can be tuned by the external bias current. The circuit also offers the following advantage features; low power consumption, no component matching conditions, and high-output impedance.

2. Fundamental Circuit Blocks

In this section, current-mode active functional blocks that will be used as fundamental circuits in filter synthesis are introduced.

2.1 Multi-Output Current Follower

Fig. 1(a) shows the basic multi-output current follower based on an npn current mirror, where i_k (k = 1, 2, ..., n) is the output signal current, and I_B is the external DC bias current. Assuming that the common-emitter current gain is

much greater than unity ($\beta >> 1$) and the dimensions of all transistors are same, we get the following relation:

$$i_k \cong i_{in} \quad . \tag{1}$$

Fig. 1(b) shows the AC small-signal equivalent circuit of Fig. 1(a), in which R_i is the input resistance of the current follower and can be expressed as :

$$R_i = \frac{V_T}{I_E} \cong \frac{V_T}{I_B} \tag{2}$$

where $V_T = kT/q$ is the thermal voltage (~26 mV at 27°C), and I_E is the DC emitter current of the diode connected transistor Q_0, which is approximately equal to I_B. Thus, from the basic circuit operation, the block diagram of the multi-output current follower shown in Fig. 1(a) can be represented as Fig. 1(c).

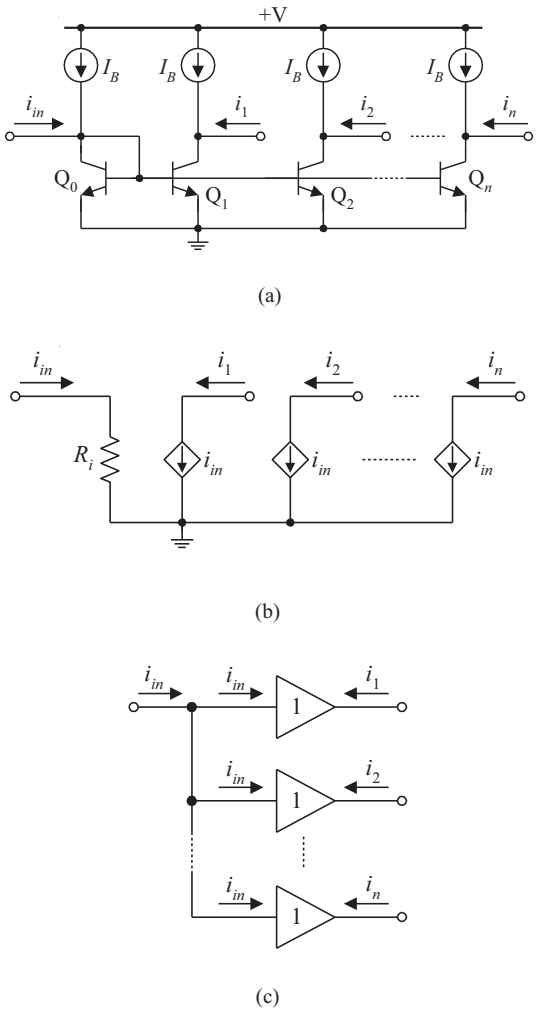

Fig. 1. Multi-output current follower; (a) transistor circuit, (b) small-signal equivalent circuit, (c) its block.

2.2 Tunable Lossy Current Integrator

Fig. 2(a) shows the basic tunable lossy current integrator. The matched transistors Q_3 and Q_4 construct a simple current mirror with capacitor C connected parallel to the mirror input. The small-signal equivalent circuit of Fig. 2(a) is shown in Fig. 2(b), where $g_{m3} = I_B/V_T$ represents the small-signal equivalent conductance of Q_3, and A is the emitter area ratio of the output transistor Q_4 to the input transistor Q_3. From the figure, it can be readily shown that the current transfer function can be given by

$$\frac{i_{o1}}{i_{in}} = \frac{g_{m3}A}{g_{m3} + sC} \quad . \tag{3}$$

According to (3), the block representation of Fig. 2(a) can be drawn in Fig. 2(c).

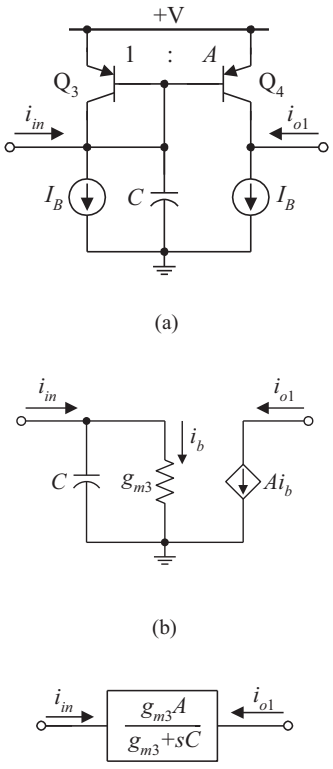

Fig. 2. Electronically tunable lossy current integrator; (a) transistor circuit, (b) small-signal equivalent circuit, (c) its block.

3. Proposed Current-Mode AP/HP Filter

The generic conceptualization of the proposed first-order filter block is shown in Fig. 3(a). As can be seen, the configuration comprises two sub-blocks: a dual-output current follower of Fig. 1(c) and a tunable lossy current integrator of Fig. 2(c). Using the circuits from Fig. 1(a) and 2(a) in the proposed filter topology of Fig. 3(a), one readily obtains the resistorless bipolar technology-based filter configuration shown in Fig. 3(b). Analysis of the proposed configuration of Fig. 3 gives the following current transfer function,

$$\frac{i_{out}}{i_{in}} = 1 - \frac{g_{m3}A}{g_{m3} + sC}. \tag{4}$$

This transfer function allows designing two different types of first-order filter realizations by setting emitter area of Q_4 (A) appropriately.

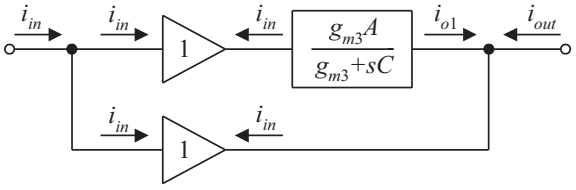

(a)

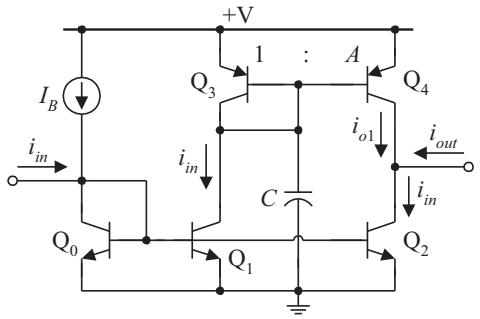

(b)

Fig. 3. Basic principle of proposed first-order current-mode AP/HP filter; (a) block diagram, (b) bipolar technology-based realization.

For A = 1, (4) becomes :

$$\frac{i_{HP}}{i_{in}} = \frac{i_{out}}{i_{in}} = 1 - \frac{g_{m3}}{g_{m3} + sC} = \frac{sC}{sC + g_{m3}}. \tag{6}$$

It is apparent from (6) that, in this case, the circuit realizes the standard transfer function of first-order HP filter.

In case that A = 2 (i_{o1} is mirrored from i_{in} with a scale factor 2), the following transfer function is obtained for the first-order AP filter response:

$$\frac{i_{AP}}{i_{in}} = \frac{i_{out}}{i_{in}} = 1 - \frac{2g_{m3}}{g_{m3} + sC} = \frac{sC - g_{m3}}{sC + g_{m3}} \tag{7}$$

with the phase response of

$$\phi = \pi - 2\tan^{-1}\left(\frac{\omega V_T C}{I_B}\right). \tag{8}$$

Both AP and HP types of first-order current-mode filter have the same following pole frequencies.

$$\omega_o = \frac{g_{m3}}{C} = \frac{I_B}{V_T C}. \tag{9}$$

Equations (8) and (9) clearly indicate that the bandwidth and phase response of the circuit in Fig. 3(b) can be easily tuned via a DC bias current I_B. Note at this point that the filter parameters are actually temperature-sensitive, because V_T is directly proportional to the absolute temperature T.

In Fig. 4, the complete circuit diagram of the proposed one in Fig. 3 is demonstrated. Variables i_{AP} and i_{HP} are the allpass and highpass current responses, respectively. Here, the current i_{AP} is realized by adding Q_5 to provide double emitter area.

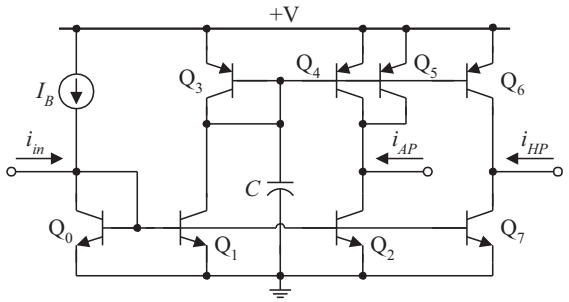

Fig. 4. Complete circuit of proposed tunable first-order current-mode AP/HP filter.

4. Non-Ideal Effects

In this section, the effects of the current mirror mismatches and transistor parasitic elements on the proposed circuit in Fig. 4 are investigated.

4.1 Effects of Current Mirror Mismatches

In ideal case, the current gain β is large enough, the transistor base currents are assumed to be zero. However, in the actual design, transistors have finite β. Therefore, the base currents cannot be ignored. Taking into account the effects of non-zero base currents in the proposed circuit of Fig. 4, the current transfer functions in (6) and (7) can respectively be rewritten as the following forms:

$$\frac{i_{HP}}{i_{in}} = (1 - \varepsilon_n)\left[\frac{sC + g_{m3}\varepsilon_p}{sC + g_{m3}}\right] \tag{10}$$

and

$$\frac{i_{AP}}{i_{in}} = (1 - \varepsilon_n)\left[\frac{sC - g_{m3}(1 - 2\varepsilon_p)}{sC + g_{m3}}\right] \tag{11}$$

where

$$\varepsilon_{n(p)} = \frac{1}{1 + \frac{\beta_{n(p)}}{4}}$$

are the current transfer errors associated with the current mirrors Q_0-Q_2, Q_7, and Q_3-Q_6, and $\beta_{n(p)}$ are the current gains of npn and pnp transistors, respectively. In practice, $\beta_{n(p)}$ usually depend on the process of integrated circuit technologies, and vary with the change in operating temperature, biasing voltage and current.

4.2 Effects of Parasitic Elements

The transistor parasitic effects on the proposed AP/HP filter are considered in this sub-section. The small-signal model of the bipolar transistor with parasitic elements is demonstrated in Fig. 5. In the equivalent circuit model, some parasitic elements are defined as: base-emitter resistance (r_π), base-emitter capacitance (C_π) and base-collector capacitance (C_μ). By using the simple small-signal model of Fig. 5 and assuming $C_\pi >> C_\mu$, the current transfer functions of Fig. 4 can be approximated as, respectively,

$$\frac{i_{HP}}{i_{in}} = K_n \left[\frac{s\left(\dfrac{C + 4C_{\pi p} + C_{\mu p}}{g_{mp} + \dfrac{4}{r_{\pi p}}} \right) + \left(\dfrac{1}{1 + \dfrac{g_{mp} r_{\pi p}}{4}} \right)}{s\left(\dfrac{C + 4C_{\pi p} + C_{\mu p}}{g_{mp} + \dfrac{4}{r_{\pi p}}} \right) + 1} \right] \tag{12}$$

and

$$\frac{i_{AP}}{i_{in}} = K_n \left[\frac{s\left(\dfrac{C + 4C_{\pi p} + 2C_{\mu p}}{g_{mp} + \dfrac{4}{r_{\pi p}}} \right) - \left(\dfrac{1 - \dfrac{4}{g_{mp} r_{\pi p}}}{1 + \dfrac{4}{g_{mp} r_{\pi p}}} \right)}{s\left(\dfrac{C + 4C_{\pi p} + 2C_{\mu p}}{g_{mp} + \dfrac{4}{r_{\pi p}}} \right) + 1} \right] \tag{13}$$

where

$$K_n = \frac{1}{1 + \dfrac{4}{g_{mn} r_{\pi n}}}, \tag{14}$$

and $g_{mn(p)}$, $r_{\pi n(p)}$, $C_{\pi n(p)}$ and $C_{\mu n(p)}$ are the g_m, r_π, C_π and C_μ of npn and pnp transistors, respectively. Since normally $C_\pi >> C_\mu$, then the circuit has the non-ideal pole frequency located at:

$$\omega_o \cong \frac{g_{mp} + \dfrac{4}{r_{\pi p}}}{C + 4C_{\pi p}} \tag{15}$$

It is observed from (14) and (15) that the effects of transistor parasitic elements produce a small deviation in the frequency responses of the proposed filter. Therefore, to obtain an ideal filter response, one should select as: $g_{mn(p)} r_{\pi n(p)} >> 4$ and $C >> 4C_{\pi p}$.

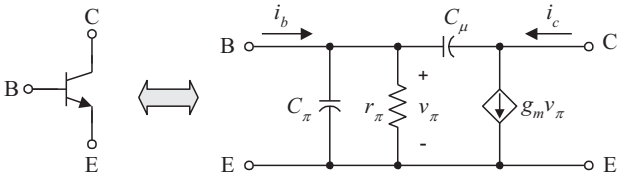

Fig. 5. Small-signal equivalent circuit of bipolar transistor.

5. Temperature Compensation

As mentioned earlier, the apparent disadvantage of the proposed filter parameters shows a strong directly related relationship with the absolute temperature. Therefore, a biasing circuit configuration to obtain temperature insensitivity will be suggested in this section.

Fig. 6 shows the basic scheme for an npn current mirror with controllable gain, where transistors Q_{1t} to Q_{4t} function as a classical Seevinck's translinear gain cell [18]-[19]. Assuming that $\beta >> 1$ and the translinear conditions are satisfied, the translinear relation that exists between their collector currents gives the output current I_O to be expressed as:

$$I_O = \frac{I_{B1} I_{B3}}{I_{B2}} \tag{16}$$

where I_{B1}, I_{B2} and I_{B3} are the external DC bias currents.

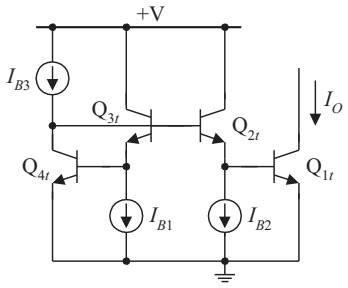

Fig. 6. npn current mirror with adjustable current gain.

Fig. 7 shows a circuit diagram of a low-voltage bipolar translinear-based dependent current source, which is obtained from the basic circuit of Fig. 6 by inserting current mirrors Q_{9t} -Q_{11t}, Q_{12t} -Q_{14t} and the resistor R. From the figure, applying the translinear principle, we have the following relations:

$$I_{C5} R + V_T \ln\left(\frac{I_{C5}}{I_{S5}}\right) + V_T \ln\left(\frac{I_{C6}}{I_{S6}}\right) = V_T \ln\left(\frac{I_{C7}}{I_{S7}}\right) + V_T \ln\left(\frac{I_{C8}}{I_{S8}}\right)$$

or

$$I_{C5} = \frac{V_T}{R} \ln\left(\frac{I_{C7} I_{C8} I_{S5} I_{S6}}{I_{C5} I_{C6} I_{S7} I_{S8}}\right). \tag{17}$$

Assuming that $I_{S5} \cong I_{S6} \cong I_{S7} \cong I_{S8}$, $I_{C7} \cong I_{C10} \cong I_{B4}$, $I_{C5} \cong I_{C8} \cong I_{O1}$ and setting $I_{C6} \cong I_{C11} \cong 0.37 I_{B4}$. Thus, (17) turns to:

$$I_{O1} = \frac{V_T}{R} \ln \alpha \tag{18}$$

where α is the ratio between emitter areas of transistors Q_{9t} and Q_{11t}, and in this case $\alpha = 1/0.37$.

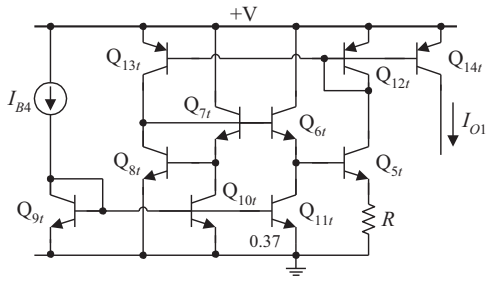

Fig. 7. Low-voltage translinear-based dependent current source.

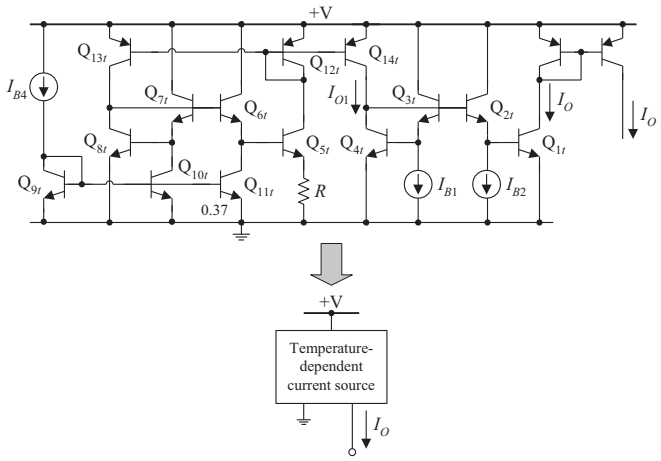

Fig. 8. Suggested biasing circuit for temperature compensation.

The schematic diagram of the suggested biasing circuit is shown in Fig. 8. The circuit consists of a basic circuit in Fig. 6 and a low-voltage translinear-based circuit in Fig. 7. Therefore, the output current I_O of the circuit can be obtained by substituting I_{O1} from (18) into I_{B3} of (16) and can be written as:

$$I_O = \frac{I_{B1} V_T}{I_{B2} R} \tag{19}$$

The above expression reveals that the output current is directly proportional to the thermal voltage V_T, which is itself directly related to the absolute temperature T, and the bias current ratio of I_{B1}/I_{B2}. Consequently, the circuit that a bias condition is strong inversely depend on the absolute temperature can be corrected by this temperature-dependent current source.

From the proposed first-order current-mode AP/HP filter in Fig. 4, it is seen that the ω_o of (9) is linearly related to the bias current I_B and inversely temperature dependent. Therefore, for the reasons given above, a biasing circuit to obtain temperature insensitivity will be required. Consider the temperature compensated filter circuit of Fig. 9, where the bias current I_B of Fig. 4 is replaced by the current source I_O from the biasing circuit of Fig. 8. Combining (9) and (19), the pole frequency f_o is again given by:

$$f_o = \left(\frac{I_{B1}}{I_{B2}}\right)\left(\frac{1}{2\pi RC}\right) \tag{20}$$

where it can be readily shown that now the f_o is insensitive to the temperature and also can be controlled electronically by changing the bias current ratio I_{B1}/I_{B2}.

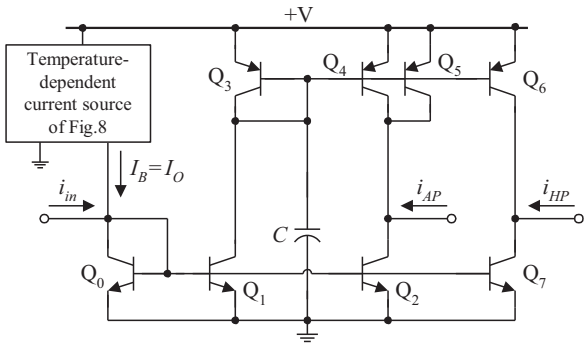

Fig. 9. Proposed tunable first-order current-mode AP/HP filter with temperature compensation.

6. Simulation Results

To verify the theoretical study, the proposed current-mode AP/HP filter in Fig. 4 was simulated using PSPICE program with the transistor model parameters PR100N (PNP) and NP100N (NPN). The circuit was supplied from DC voltage of +V = 1.5 V. The DC bias current I_B = 26 μA and capacitor C = 1 nF resulting in the pole frequency of $f_o \cong 159$ kHz were chosen. The simulated frequency responses of the propose AP filter is shown in Fig. 10, which demonstrates a constant unity gain for several decades between 1 kHz and 10 MHz approximately. For the above designed component values, the time-domain response of the proposed AP filter is shown in Fig. 11. A 10-μA peak sinusoidal input current with a frequency of 159 kHz was applied to the filter, showing a 84° phase-shift in the output to a sinusoidal input of the filter. This result is close to the expected value, which is equal to 90°. The total harmonic distortion (THD) variation at the AP output with respect to the amplitude of input signal current was also studied, and the results are shown in Fig.12. The results show that the THD for a sinusoidal input signal level (few μA to 20 μA) variation at 159 kHz is found within 8 %. The total power consumption was found to be 169 μW, which is a considerably low value.

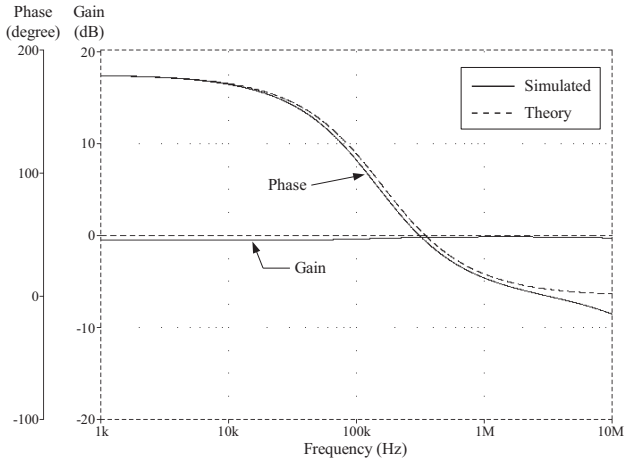

Fig. 10. Simulated gain and phase responses of the proposed AP filter in Fig.4.

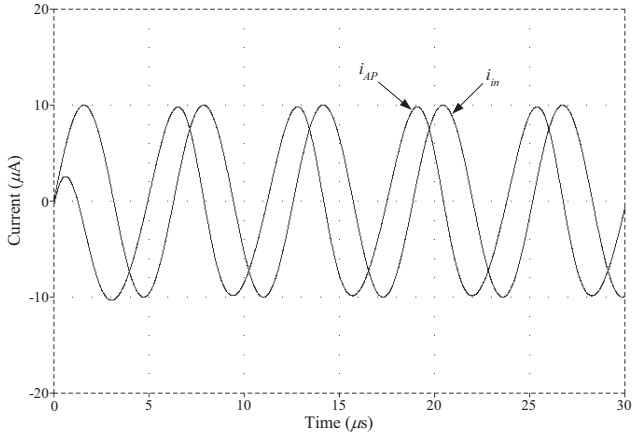

Fig. 11. Time-domain response of the proposed AP filter at operating frequency of 159 kHz.

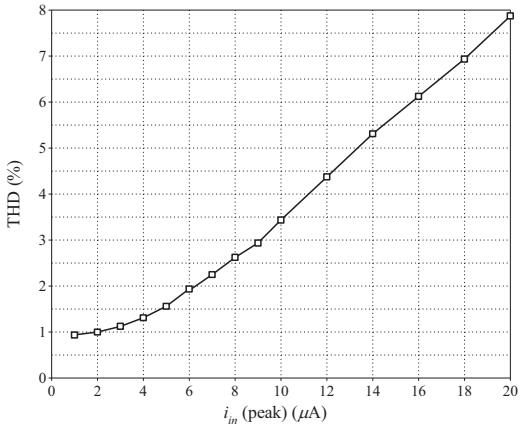

Fig. 12. THD variation with applied input current signal amplitude.

To evaluate the effects of the active and passive component tolerances on the filter performance, Monte-Carlo statistical analysis is performed. In this study, 200 simulation runs with 10 % Gaussian deviation on capacitor and g_{m3} values are applied to the proposed filter. Simulation results of Monte-Carlo PSPICE analysis are given in Figs. 13 and 14, respectively. They demonstrate that the proposed filter works well against component tolerances.

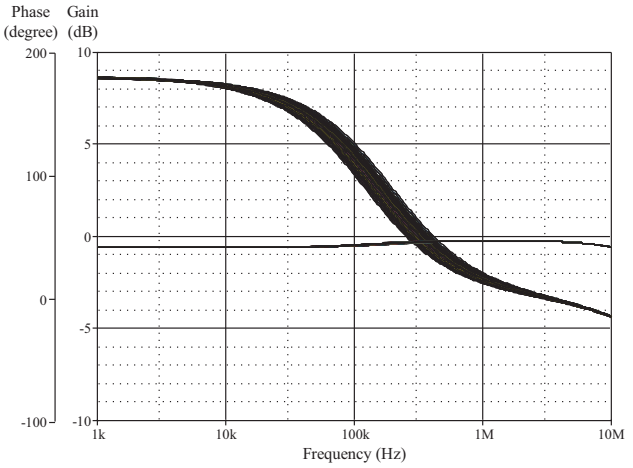

Fig. 13. Monte-Carlo analysis of the AP frequency response for 10 % Gaussian deviation in the capacitor value.

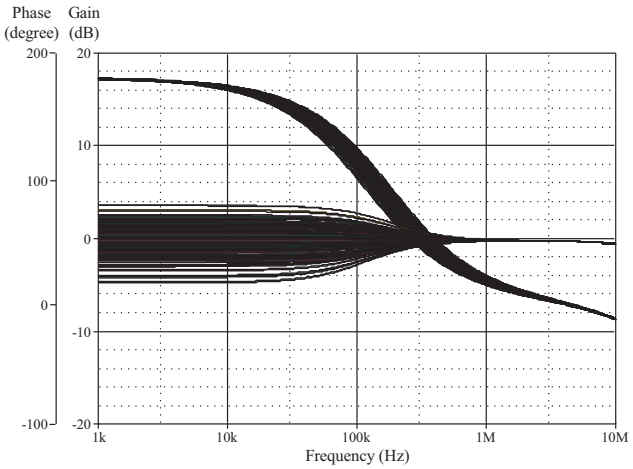

Fig. 14. Monte-Carlo analysis of the AP frequency response for 10 % Gaussian deviation in the g_{m3}-value.

The electronic tuning aspect of the proposed HP filter is shown in Fig. 15, in which the gain responses for three different values of I_B are given. As expected, the corresponding pole frequency is varied from 61 kHz, over 159 kHz to 306 kHz for a variation of I_B from 10 μA, 26 μA to 50 μA, respectively. This confirms that the proposed circuit is electronically adjustable by controlling the bias current I_B.

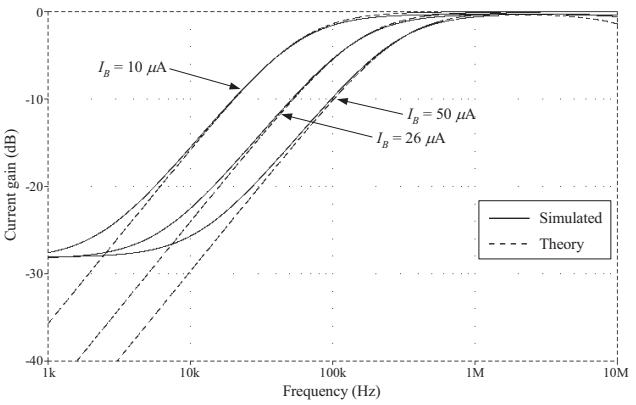

Fig. 15. Plot of magnitude characteristics of the HP filter with various I_B.

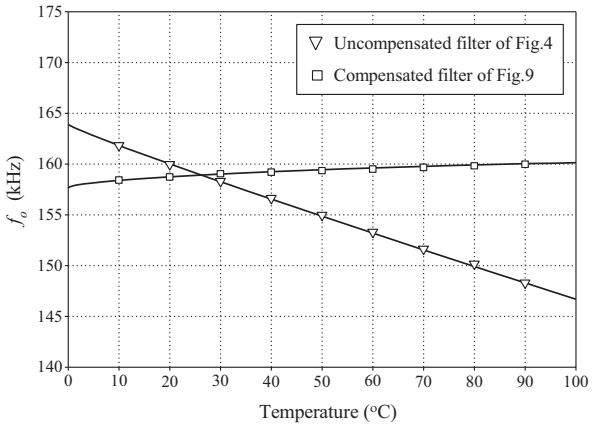

Fig. 16. Variation of f_o against temperature.

The dependency of the pole frequency f_o on temperature was also simulated. For the temperature compensated filter circuit of Fig. 9, we set I_{B1} = 5 μA, $I_{B2} = I_{B4}$ = 50 μA, R = 100 Ω and varying the temperature from 0 °C to 100 °C. The simulated f_o against temperature are illustrated in Fig.16, which display the values of f_o for the case of the uncompensated circuit in Fig. 4 and compensated circuit in Fig. 9. The relative sensitivities of f_o with respect to temperature of the uncompensated and compensated circuits, which is given by

$$S_T^{f_o} = (\partial f_o / f_o)/(\partial T/T),$$

are approximately equal to 75.15×10^{-3} and 17.55×10^{-3}, respectively. It is clearly seen that the compensated filter gives much lower temperature sensitivity.

7. Experimental Test Results

In order to further verify the proper operation of the proposed AP/HP filter in Fig. 4, the circuit has also been tested experimentally. To perform the measurements of the proposed circuit, the readily available transistor arrays CA 3096 by Intersil have been used, and the measured circuit was extended by voltage-to-current and current-to-voltage converters realized by commercially available CFOA AD844s with ±5V dc power supply voltages. The circuit configuration used for experimental test is shown in Fig. 17. The experiments have been performed with $R_1 = R_2 = R_3 = R_4$ = 10 kΩ, C = 33 nF and V_B = 3 V (I_B = 300 μA), which ensured that $f_o \cong$ 55.65 kHz according to (9). In measurements, v_{in} = 0.5 sin ($2\pi f$) V (peak) was applied to the circuit. Fig.18 shows the experimental values for the AP gain and phase responses with respect to frequency. The experimental test results for time-domain waveforms and Lissajous figure with 90° phase difference at the pole frequency, which verify the circuit as a phase shifter, are demonstrated in Figs. 19 and 20, respectively. Fig. 21 also shows the measured output spectrum of AP filter.

8. Conclusion

A very compact circuit, consisting of eight bipolar transistors and one grounded capacitor, has been presented to implement first-order current-mode AP and HP filters. It features low-voltage operation, and smaller power consumption. The circuit also provides an ability to vary its important parameters by means of the external bias current. In the absence of the external resistor, easily integrable version of an electronically tunable first-order current-mode filter block is obtainable. In addition, a synthesis method of a low-voltage bipolar translinear-based biasing circuit with a current linearly proportional to absolute temperature is also introduced and applied to compensate the temperature sensitivity of the proposed filter. We have shown through simulation and experimental results that the operation of the developed circuits is agreement with the theory.

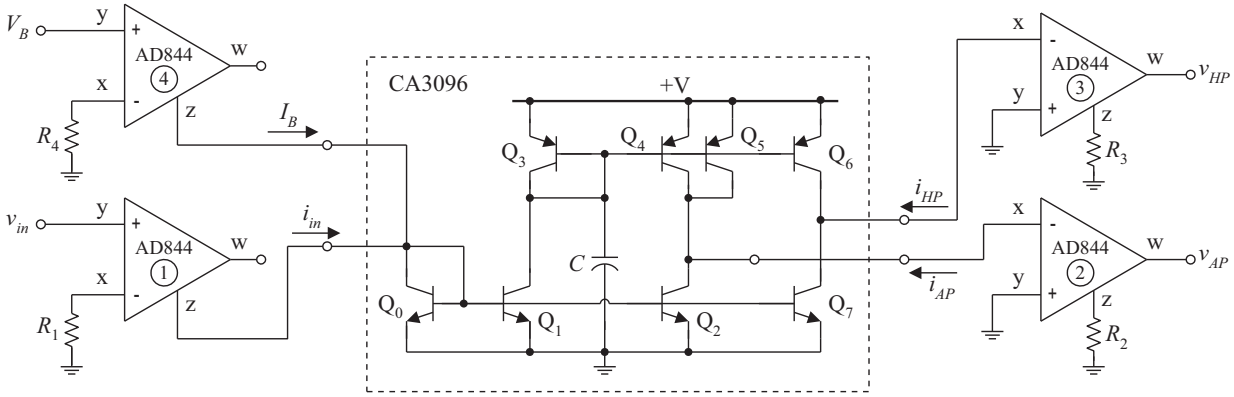

Fig. 17. AP/HP filter configuration used for experimental test.

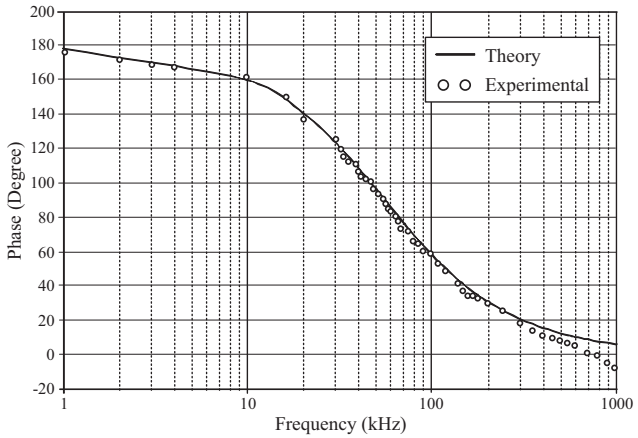

(a)

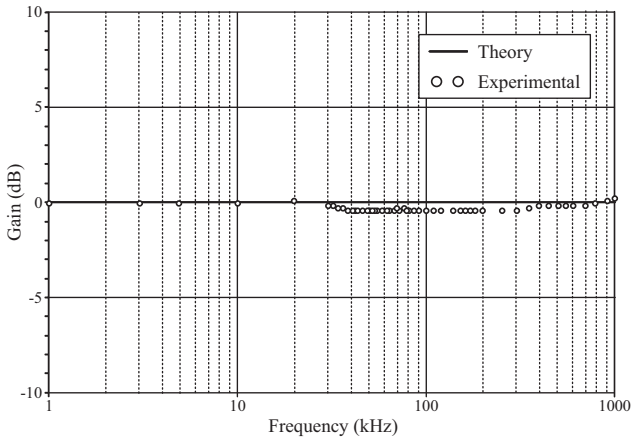

(b)

Fig. 18. Experimental results for the AP filter of Fig.17. (a) gain response, (b) phase response.

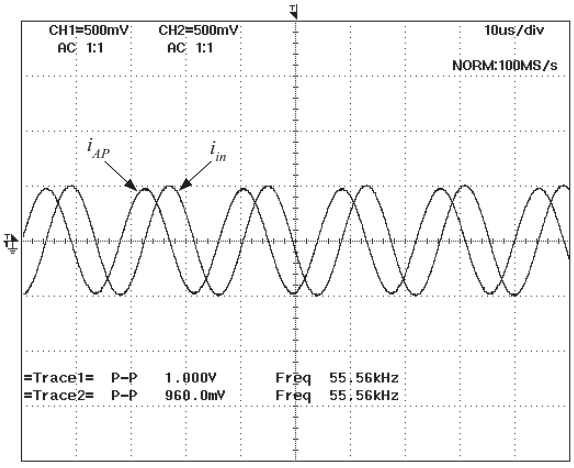

Fig. 19. Measured input/output waveforms for the proposed AP filter at the pole frequency.

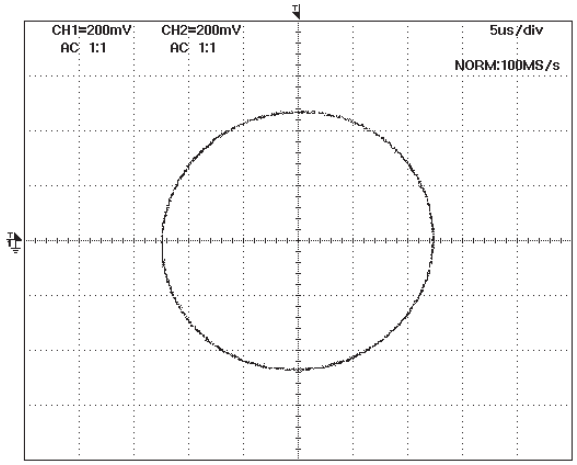

Fig. 20. Lissajous figure for the proposed AP filter at the pole frequency.

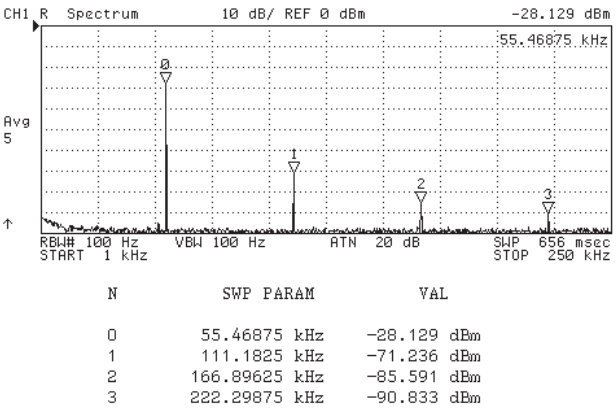

N	SWP PARAM	VAL
0	55.46875 kHz	-28.129 dBm
1	111.1825 kHz	-71.236 dBm
2	166.89625 kHz	-85.591 dBm
3	222.29875 kHz	-90.833 dBm

Fig. 21. Measured spectral plot for the proposed AP filter at the pole frequency.

Acknowledgement

This research work is supported by Faculty of Engineering, King Mongkut's Institute of Technology Ladkrabang (KMITL). The author would like to thank Mr. Jetsdaporn Satansup for his performing Monte-Carlo statistical analysis, and Mr. Danucha Prasertsom for recording experimental test data.

References

[1] HIGASHIMURA, M., FUKUI, Y. Realization of current-mode all-pass networks using a current conveyor. *IEEE Transactions on Circuits and Systems*, 1990, vol. 37, no. 5, p. 660 - 661.

[2] HIGASHIMURA, M. Current-mode first-order allpass filter using FTFN with grounded capacitor. *Electronics Letters*, 1991, vol. 27, no. 13, p. 1182 - 1183.

[3] MAHESHWARI, S., KHAN, I. A. Simple first-order translinear-C current-mode all-pass sections. *International Journal of Electronics*, 2003, vol. 90, no. 2, p. 79 - 85.

[4] MAHESHWARI, S. New voltage and current-mode APS using current controlled conveyors. *International Journal of Electronics*, 2004, vol. 91, no. 12, p. 735 - 743.

[5] KILINC, S., CAM, U. Current-mode first-order allpass filter employing single current operational amplifier. *Analog Integrated Circuits and Signal Processing*, 2004, vol. 41, no. 1, p. 47 - 53.

[6] MINAEI, S., IBRAHIM, M. A. General configuration for realizing current-mode first-order all-pass filter using DVCC. *International Journal of Electronics*, 2005, vol. 92, no. 6, p. 347 - 356.

[7] HORNG, J. W., HOU, C. L., CHANG, C. M., CHUNG, W. Y., LIU, H. L., LIN, C. T. High output impedance current-mode first-order allpass networks with four grounded components and two CCIIs. *International Journal of Electronics*, 2006, vol. 93, no. 9, p. 613 - 621.

[8] MAHESHWARI, S. Novel cascadable current-mode first order all-pass sections. *International Journal of Electronics*, 2007, vol. 94, no. 11, p. 995 - 1003.

[9] METIN, B., PAL, K., CICEKOGLU, O. All-pass filter for rich cascadability options easy IC implementation and tunability. *International Journal of Electronics*, 2007, vol. 94, no. 11, p. 1037 - 1045.

[10] OZTAYFUN, S., KILINC, S., CELEBI, A., CAM, U. A new electronically tunable phase shifter employing current-controlled current conveyors. *International Journal of Electronics and Communication (AEU)*, 2008, vol. 62, p. 228 - 231.

[11] TANGSRIRAT, W., PUKKALANUN, T., SURAKAMPONTORN, W. Resistorless realization of current-mode first-order allpass filter using current differencing transconductance amplifyers. *Microelectronics Journal*, 2010, vol. 41, no. 2-3, p. 178 - 183.

[12] ARSLANALP, R., YUCE, E. A BJT technology-based current-mode tunable all-pass filter. *Microelectronics Journal*, 2009, vol. 40, no. 6, p. 921 - 927.

[13] LAHIRI, A. New CMOS-based resistor-less current-mode first-order all-pass filter using only ten transistors and one external capacitor. *Radioengineering*, 2011, vol. 20, no. 3, p. 638 - 643.

[14] ARSLANALP, R., TOLA, A. T., YUCE, E. Novel resistorless first-order current-mode universal filter employing a grounded capacitor. *Radioengineering*, 2011, vol. 20, no. 3, p. 656 - 665.

[15] YUCE, E., MINAEI, S., HERENCSAR, N., KOTON, J. Realization of first-order current-mode filters with low number of MOS transistors. *Journal of Circuits, Systems and Computers,* 2013, vol. 22, no. 1, p. 1250071.

[16] YILDIZ, H. A., OZOGUZ, S., TOKER, A., CICEKOGLU, O. On the realization of MOS-only allpass filters. *Circuits, Systems and Signal Processing*, 2013, vol. 32, no. 3, p. 1455 - 1465.

[17] PROMMEE, P., WONGPROMMOON, N. Log-domain all-pass filter-based multiphase sinusoidal oscillators. *Radioengineering*, 2013, vol. 22, no.1, p. 14 - 23.

[18] GILBERT, B. Translinear circuit: A proposed classification. *Electronics Letters*, 1975, vol. 11, p. 14 - 16.

[19] SEEVINCK, E. Companding current-mode integrator: A new circuit principle for continuous-time monolithic filters. *Electronics Letters*, 1990, vol. 26, no. 24, p. 2046 - 2047.

About Author …

Worapong TANGSRIRAT was born in Uthaithani, Thailand, in 1968. He received M.Eng. and D.Eng. degrees in Electrical Engineering from Faculty of Engineering, King Mongkut's Institute of Technology Ladkrabang (KMITL), Bangkok, Thailand in 1997 and 2003, respectively. Currently, he is an Associate Professor in electrical engineering at the same institute. His research interests are mainly in integrated circuit design, analog signal processing, current-mode circuits, and active filter design.